

SUPPLEMENTAL MATERIAL

Dynamical criticality in driven systems: Non-perturbative results, microscopic origin and direct observation

Carlos Pérez-Espigares,¹ Federico Carollo,¹ Juan P. Garrahan,¹ and Pablo I. Hurtado²

¹*School of Physics and Astronomy, and Centre for the Mathematics and Theoretical Physics of Quantum Non-Equilibrium Systems, University of Nottingham, Nottingham, NG7 2RD, UK*

²*Departamento de Electromagnetismo y Física de la Materia, and Institute Carlos I for Theoretical and Computational Physics, Universidad de Granada, Granada 18071, Spain*

CONTENTS

I. A crash course on MFT	2
II. Steady state for the $1d$ open WASEP	4
III. Joint mass-current fluctuations in the $1d$ open WASEP	5
A. Two pairs of complex conjugate roots	7
B. Two real roots, one pair of complex conjugate roots	8
C. Four real roots	11
IV. Instanton solution, Maxwell-like construction and violation of additivity principle	15
V. Spectral analysis of the dynamical generator and metastable manifold	17
A. Non-degenerate largest eigenvalue (PH symmetric phase)	18
B. Degenerate largest eigenvalue (PH symmetry-broken phase)	18
References	19

In this Supplemental Material we solve the macroscopic fluctuation theory (MFT) equations for the joint current and mass fluctuations of the one-dimensional ($1d$) weakly asymmetric simple exclusion process (WASEP) coupled to boundary particle reservoirs at arbitrary densities or chemical potentials. This model belongs in a large class of driven diffusive systems of theoretical and technological interest. MFT [1] provides a detailed description of dynamical fluctuations in general driven diffusive systems, starting from the hydrodynamic evolution equation for the system of interest and the sole knowledge of two transport coefficients, which can be measured experimentally. In particular, MFT offers explicit predictions for the large-deviation functions (LDFs) which characterize the fluctuations of different observables, as well as the associated trajectories in phase space responsible of these fluctuations.

After a brief but self-consistent presentation of MFT in §I and a characterization of the nonequilibrium steady state of the $1d$ open WASEP under arbitrary driving (see §II), we proceed to solve analytically in §III the MFT equations for the joint mass-current statistics of this model, understanding along the way the symmetry-breaking dynamical phase transition described in the main text. Key to this calculation is the additivity conjecture [2], which assumes that the optimal trajectories responsible of a trajectory are time-independent. We explore in §IV the possibility of additivity violations in the form of time-dependent, instantonic solutions to the MFT equations in regimes where the joint current-mass LDF becomes non-convex. Finally, we study in §V from a microscopic point of view the DPT found at the macroscopic level, using in particular the quantum Hamiltonian formalism for the master equation and the tilted dynamical generator.

I. A CRASH COURSE ON MFT

We hence consider systems described at the mesoscopic level by a continuity equation of the form

$$\partial_t \rho + \partial_x j = 0, \quad (\text{S1})$$

where $\rho(x, t)$ and $j(x, t)$ are the density and current fields, respectively, and $x \in [0, 1]$ and t are the macroscopic space and time variables, obtained after a diffusive scaling limit such that $x = \tilde{x}/L$ and $t = \tilde{t}/L^2$, with \tilde{x} and \tilde{t} the equivalent microscopic variables and L the system size in natural units. The system is coupled at the boundaries to particle reservoirs at densities $\rho_{L,R}$, so the boundary conditions for the density field are $\rho(0, t) = \rho_L$ and $\rho(1, t) = \rho_R \forall t$. The current field in eq. (S1) is in general a fluctuating quantity, and can be written as

$$j(x, t) = -D(\rho)\partial_x \rho(x, t) + \sigma(\rho)E + \xi(x, t). \quad (\text{S2})$$

The first two terms in the rhs are just Fick's law, which express the proportionality of the current to the density gradient and the external field E , with $D(\rho)$ and $\sigma(\rho)$ the diffusivity and mobility transport coefficients (which might be nonlinear functions of the local density). The last term $\xi(x, t)$ is a *weak* Gaussian white noise, such that

$$\langle \xi(x, t) \rangle = 0, \quad \langle \xi(x, t) \xi(x', t') \rangle = \frac{\sigma(\rho)}{L} \delta(x - x') \delta(t - t'). \quad (\text{S3})$$

This noise term accounts for all fast degrees of freedom which are integrated out in the coarse-graining procedure which results in the mesoscopic hydrodynamic description (S1)-(S2). After some relaxation time, a system described by the above set of equations reaches a nonequilibrium steady state characterized by a (typically inhomogeneous) density profile $\rho_{\text{st}}(x)$ compatible with the above boundary conditions, and a nonzero average current $\langle q \rangle = -D(\rho_{\text{st}})\partial_x \rho_{\text{st}} + \sigma(\rho_{\text{st}})E$ constant across space. Note that, for WASEP, the two key transport coefficients are $D(\rho) = \frac{1}{2}$ and $\sigma(\rho) = \rho(1 - \rho)$ [3, 4], and Section §II below describes the steady-state solution of the above hydrodynamic equations for the $1d$ open WASEP.

A simple path integral calculation starting from Eqs. (S1)-(S2) then shows that the probability of a given field trajectory $\{\rho, j\}_0^\tau$ obeys a large deviation principle of the form $P(\{\rho, j\}_0^\tau) \sim \exp(-L\mathcal{I}_\tau[\rho, j])$, with an action given by [1, 5, 6]

$$\mathcal{I}_\tau[\rho, j] = \int_0^\tau dt \int_0^1 dx \frac{[j + D(\rho)\partial_x \rho - E\sigma(\rho)]^2}{2\sigma(\rho)}, \quad (\text{S4})$$

with $\rho(x, t)$ and $j(x, t)$ coupled via the continuity equation $\partial_t \rho + \partial_x j = 0$ (in any other case $\mathcal{I}_\tau[\rho, j] \rightarrow \infty$). We are interested here in the joint statistics for fluctuations of the spacetime-integrated current q and mass m . These two empirical observables are defined as

$$q = \frac{1}{\tau} \int_0^\tau dt \int_0^1 dx j(x, t), \quad (\text{S5})$$

$$m = \frac{1}{\tau} \int_0^\tau dt \int_0^1 dx \rho(x, t). \quad (\text{S6})$$

The probability of observing a given q and m can now be written as a path integral over all possible trajectories $\{\rho, j\}_0^\tau$, weighted by its probability measure $P(\{j, \rho\}_0^\tau)$, and restricted to those trajectories compatible with the values of q and m in Eqs. (S5) and (S6), respectively, the continuity equation (S1) at every point of space and time, and the fixed boundary conditions for the density field. For long times and large system sizes, this sum over trajectories is dominated by the associated saddle point and scales as $P(m, q) \sim \exp\{-\tau LG(m, q)\}$, where $G(m, q)$ is the mass-current large deviation function (LDF) given by

$$G(m, q) = \lim_{\tau \rightarrow \infty} \frac{1}{\tau} \min_{\{\rho, j\}_0^\tau} \mathcal{I}_\tau(\rho, j). \quad (\text{S7})$$

The density and current fields solution of this variational problem, denoted here as $\rho_{m,q}(x, t)$ and $j_{m,q}(x, t)$, can be interpreted as the optimal trajectory the system follows in order to sustain a long-time mass and current joint fluctuation, and are in general time-dependent.

However, in most applications of MFT to study fluctuations of time-integrated observables in open systems, such as (S5)-(S6), it has been found that the optimal trajectory $\{\rho_{m,q}, j_{m,q}\}_0^\tau$ is indeed *time-independent*. Physically this means that, in order to sustain a given mass-current long-time fluctuation, the system of interest settles after a

negligible initial transient into a time-independent state (possibly followed by an equally negligible final transient). This property, known as Additivity Principle in literature [1, 2, 7–19], strongly simplifies the variational problem at hand. In particular, the mass-current LDF now reads

$$G(m, q) = \min_{\rho(x)} \int_0^1 dx \frac{[q + D(\rho)\rho'(x) - \sigma(\rho)E]^2}{2\sigma(\rho)}. \quad (\text{S8})$$

The optimal density profile solution of this simpler variational problem, $\rho_{m,q}(x)$, is subject to the additional constraint

$$m = \int_0^1 \rho_{m,q}(x) dx, \quad (\text{S9})$$

and the optimal current field is simply $j_{m,q}(x) = q$ due to the continuity equation (S1) and the time-independence of the dominant trajectory. The integral constraint (S9) can be implemented using a Lagrange multiplier λ which will be fixed *a posteriori* to enforce the constraint. We hence define a new function

$$G(\lambda, q) = \min_{\rho(x)} \int_0^1 dx \left\{ \frac{[q + D(\rho)\rho'(x) - \sigma(\rho)E]^2}{2\sigma(\rho)} - \lambda\rho(x) \right\}. \quad (\text{S10})$$

The optimal density field for this variational problem is the solution of the following Euler-Lagrange equation

$$q^2 \left(\frac{1}{2\sigma(\rho)} \right)' + \frac{E^2}{2} \sigma'(\rho) - \rho''(x) \frac{D(\rho)^2}{\sigma(\rho)} - \rho'(x)^2 \left(\frac{D(\rho)^2}{2\sigma(\rho)} \right)' = \lambda, \quad (\text{S11})$$

where the $'$ means derivative with respect to the argument, e.g. $\sigma'(\rho) = \frac{d\sigma(\rho)}{d\rho}$ and $\rho'(x) = \frac{d\rho(x)}{dx}$. Multiplying both sides of this equation by $\rho'(x)$, we arrive easily to

$$\frac{d}{dx} \left[\frac{q^2}{2\sigma(\rho)} - \lambda\rho(x) + \frac{E^2}{2} \sigma(\rho) - \rho'(x)^2 \frac{D(\rho)^2}{2\sigma(\rho)} \right] = 0, \quad (\text{S12})$$

which can be trivially integrated once to yield

$$D(\rho)^2 \left(\frac{d\rho(x)}{dx} \right)^2 = q^2 + 2(K - \lambda\rho)\sigma(\rho) + E^2\sigma(\rho)^2, \quad (\text{S13})$$

where K is an integration constant which allows us to fix the correct boundary condition at one of the two ends, $\rho_{\lambda,q}(0) = \rho_L$ and $\rho_{\lambda,q}(1) = \rho_R$ (the other boundary value is given to solve the previous first-order differential equation). Interestingly, the optimal density field solution of this differential equation does not depend on the sign of the current q or the external field E , as they both appear squared in Eq. (S13). This fact is ultimately a macroscopic manifestation of the time-reversibility of microscopic dynamics. The value of the Lagrange multiplier $\lambda = \lambda(m, q)$ can be now fixed by imposing that the total mass associated to the solution $\rho_{\lambda,q}(x)$ of the above differential equation is just m , i.e.

$$m = \int_0^1 \rho_{\lambda,q}(x) dx. \quad (\text{S14})$$

Our aim in the following sections is to solve this variational problem for the 1d open WASEP, for which the key transport coefficients are $D(\rho) = 1/2$ and $\sigma(\rho) = \rho(1-\rho)$. However, before proceeding with the analysis of fluctuations, we focus briefly on the steady state behavior.

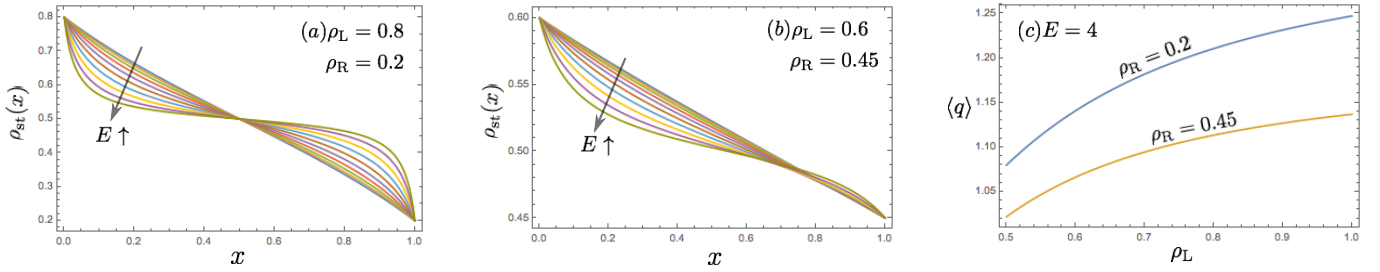


FIG. S1. (a) Steady-state density profile $\rho_{\text{st}}(x)$ for the 1d open WASEP for a symmetric gradient with boundary densities $\rho_L = 0.8$ and $\rho_R = 0.2$, and external fields $E \in [1, 50]$ increasing as $E_k = 50^{k/10}$ with $k \in [0, 10]$. (b) Same results as in (a), but for an asymmetric gradient with boundary densities $\rho_L = 0.6$ and $\rho_R = 0.45$. (c) Steady state current $\langle q \rangle$ vs ρ_L for external field $E = 4$ and two right boundary densities, namely $\rho_R = 0.2$ and $\rho_R = 0.45$.

II. STEADY STATE FOR THE 1d OPEN WASEP

In this section we derive the steady state current $\langle q \rangle$ and density profile $\rho_{\text{st}}(x)$ for the 1d open WASEP driven by an arbitrary external density gradient and possibly by an additional external field E . These steady state properties are given by Fick's law, which for $D(\rho) = 1/2$ and $\sigma(\rho) = \rho(1 - \rho)$ simply reads

$$\langle q \rangle = -\frac{1}{2} \frac{d\rho_{\text{st}}(x)}{dx} + E\rho_{\text{st}}(x)[1 - \rho_{\text{st}}(x)], \quad (\text{S15})$$

with boundary conditions $\rho_{\text{st}}(0) = \rho_L$ and $\rho_{\text{st}}(1) = \rho_R$. The previous equation can be easily solved

$$x = \int_{\rho_L}^{\rho_{\text{st}}(x)} \frac{d\rho}{2[E\rho(1 - \rho) - \langle q \rangle]} = -\frac{1}{\theta} \tan^{-1} \left(\frac{E}{\theta} (2\rho - 1) \right) \Bigg|_{\rho_L}^{\rho_{\text{st}}(x)} \equiv -\frac{1}{\theta} \mathcal{T}_\theta(\rho) \Bigg|_{\rho_L}^{\rho_{\text{st}}(x)},$$

with the definitions $\theta \equiv \sqrt{E(4\langle q \rangle - E)}$ and $\mathcal{T}_\theta(\rho) \equiv \tan^{-1} \left(\frac{E}{\theta} (2\rho - 1) \right)$. Equivalently

$$x = \frac{1}{\theta} [\mathcal{T}_\theta(\rho_L) - \mathcal{T}_\theta(\rho_{\text{st}}(x))].$$

By imposing now that $\rho_{\text{st}}(1) = \rho_R$, we obtain an implicit equation for the constant θ , i.e.

$$\theta = \mathcal{T}_\theta(\rho_L) - \mathcal{T}_\theta(\rho_R).$$

This equation for $\theta(\rho_L, \rho_R, E)$ cannot be solved analytically in general. However, it might be solved numerically for every external parameter 3-tuple (ρ_L, ρ_R, E) . From this solution one can obtain the steady-state current

$$\langle q \rangle = \frac{1}{4} \left(E + \frac{\theta^2}{E} \right) \quad (\text{S16})$$

and the stationary density profile

$$\rho_{\text{st}}(x) = \frac{1}{2} \left\{ 1 + \frac{\theta}{E} \tan[\mathcal{T}_\theta(\rho_L) - \theta x] \right\}. \quad (\text{S17})$$

Fig. S1 shows steady-state profiles and stationary currents for different values of (ρ_L, ρ_R, E) .

III. JOINT MASS-CURRENT FLUCTUATIONS IN THE 1d OPEN WASEP

We now return to our original problem of determining the optimal density field associated to a mass-current fluctuation in the 1d open WASEP. The governing differential equation (S13) reads in this case

$$\frac{1}{4} \left(\frac{d\rho}{dx} \right)^2 = q^2 + 2(K - \lambda\rho)\rho(1 - \rho) + E^2\rho^2(1 - \rho)^2, \quad (\text{S18})$$

with boundary conditions $\rho(0) = \rho_L$ and $\rho(1) = \rho_R$. Without loss of generality, we assume from now on that $\rho_L \geq \rho_R$ and $E > 0$; equivalent results to those described below hold in other situations. Note also that the case $E = 0$ results in a simpler problem lacking any dynamical phase transition [20], so it won't be studied here. The rhs of Eq. (S18) defines a fourth-order polynomial in ρ ,

$$\pi_0(\rho) \equiv q^2 + 2(K - \lambda\rho)\rho(1 - \rho) + E^2\rho^2(1 - \rho)^2 \equiv E^2\pi(\rho), \quad (\text{S19})$$

whose roots will play a key role in the analysis of possible solutions. In particular, the real roots of $\pi(\rho)$ (equivalently $\pi_0(\rho)$) define the possible extrema of the optimal density field, though as we discuss next not all real roots correspond necessarily to extrema of the profile.

A first observation is that, for $\rho_L > \rho_R$, no (local) extrema of the optimal profile $\rho_{\lambda,q}(x)$ can lie within the ρ -interval (ρ_R, ρ_L) . To see why, let's assume for a moment that there exists a local extremum $\rho_a \in (\rho_R, \rho_L)$, i.e. a real root $\rho_a \in \mathbb{R}$ such that $\pi(\rho_a) = 0$ and $\pi'(\rho_a) \neq 0$. If $\rho_a = \rho(x_a)$ is a local maximum, it must be reached from below from both sides (as $x \rightarrow x_a^\pm$), and this is not possible since $\rho_L > \rho_a$. Equivalently, if ρ_a is a local minimum it should be reached from above from both sides, and this is again not possible because $\rho_R < \rho_a$. Hence no local extrema of the density profile can lie in the interval (ρ_R, ρ_L) . Similarly, only one maximum can exist above ρ_L . Indeed, if two maxima $\rho_a > \rho_b > \rho_L$ exist (one local, the other global), they must be separated by a local minimum $\rho_c > \rho_L$. By definition, this local minimum must be reached from above from both sides, and this is again impossible since $\rho_L < \rho_c$. An equivalent argument shows that only one minimum can exist below ρ_R . Moreover, a numerical analysis of the differential equation (S18) shows that no inflection points, for which $\pi(\rho) = 0 = \pi'(\rho)$ simultaneously, are to be expected in the solutions, so we can safely assume that only maxima and minima are possible. These arguments therefore suggest that the optimal density profile solution of the Eq. (S18) can be either (a) monotonous, or contain (b) a single maximum, (c) a single minimum, or at most (d) one maximum and one minimum.

Before embarking on the general solution of the differential equation (S18), let us summarize the global solution strategy. As we will show below, the resulting density profile can be written as a rational function of Jacobi elliptic functions (either sn, cn or tn Jacobi functions [21], depending on the root structure of the polynomial $\pi(\rho)$ defined above). This density profile will be a parametric function of the current q and the external field E , as well as the constants K and λ , i.e. $\rho(x) = \rho(x; q, E, K, \lambda)$. These two latter constants must be fixed by imposing simultaneously the correct right boundary density ρ_R and the total mass m , i.e.

$$\rho(x=1; q, E, K, \lambda) = \rho_R, \quad \int_0^1 \rho(x; q, E, K, \lambda) dx = m. \quad (\text{S20})$$

Although we find below explicit solutions for $\rho(x; q, E, K, \lambda)$, the simultaneous solution of the previous equations requires numerical methods to determine the values of K and λ associated to a joint fluctuation of the current q and mass m under external field E . Moreover, the lack of intuition about the possible values of the constants K and λ for a given set of parameters (m, q, E) calls for an alternative codification of these two constants in terms of more physical quantities. In particular, defining $\rho'_{L,R}(m, q, E) \equiv \rho'(x=0, 1)$ as the slope of the optimal density profile at the left (L) and right (R) boundary, respectively, which depend on the external parameters (m, q, E) , we can see from Eq. (S18) that

$$\frac{1}{4}(\rho'_{L,R})^2 = q^2 + 2(K - \lambda\rho_{L,R})\rho_{L,R}(1 - \rho_{L,R}) + E^2\rho_{L,R}^2(1 - \rho_{L,R})^2, \quad (\text{S21})$$

which allows to write the constants K and λ in terms of the more intuitive boundary slopes $\rho'_{L,R}(m, q, E)$, i.e.

$$K(m, q, E) = \frac{\Lambda_R(m, q, E)\rho_L - \Lambda_L(m, q, E)\rho_R}{\rho_L - \rho_R}, \quad \lambda(m, q, E) = \frac{\Lambda_R(m, q, E) - \Lambda_L(m, q, E)}{\rho_L - \rho_R}, \quad (\text{S22})$$

where we have defined

$$\Lambda_{L,R}(m, q, E) \equiv \frac{\frac{1}{4}(\rho'_{L,R})^2(m, q, E) - q^2 - E^2\rho_{L,R}^2(1 - \rho_{L,R})^2}{2\rho_{L,R}(1 - \rho_{L,R})}. \quad (\text{S23})$$

Hence, for a given external field E and fixed values of the current q and the mass m , one has to find numerically the slopes $\rho'_{L,R}(m, q, E)$ such that

$$\rho(x=1; q, E, \rho'_L, \rho'_R) = \rho_R, \quad \int_0^1 \rho(x; q, \rho'_L, \rho'_R) dx = m, \quad (\text{S24})$$

where $\rho(x; q, E, \rho'_L, \rho'_R)$ is the optimal profile solution of our variational problem. Recalling now that $\rho_L \geq \rho_R$, it is interesting to note that fixing the sign of the boundary slopes $\rho'_{L,R}(m, q, E)$ determines whether the resulting profiles is either monotonous ($\rho'_L < 0, \rho'_R < 0$) or exhibits a single maximum ($\rho'_L > 0, \rho'_R < 0$), a single minimum ($\rho'_L < 0, \rho'_R > 0$), or one maximum and one minimum ($\rho'_L > 0, \rho'_R > 0$; we discuss below the reason why the maximum comes before the minimum).

We turn now to the explicit solution of the ordinary differential equation (S18), which can be written as $\rho'(x) = \pm 2|E|\sqrt{\pi(\rho)}$, where the sign depends on the section of the profile analyzed. Since $\rho_L \geq \rho_R$, monotonous profiles have $\rho'(x) \leq 0 \forall x \in [0, 1]$, and the differential equation can be integrated to yield

$$2|E|x = \int_{\rho(x)}^{\rho_L} \frac{d\rho}{\sqrt{\pi(\rho)}} \quad (\text{monotonous profile}). \quad (\text{S25})$$

For optimal profiles containing a single maximum $\rho_+ = \rho(x_+)$, such that $\pi(\rho_+) = 0$, we have $\rho'(x) = +2|E|\sqrt{\pi(\rho)}$ $\forall x \in [0, x_+]$ and $\rho'(x) = -2|E|\sqrt{\pi(\rho)}$ $\forall x \in [x_+, 1]$, and hence

$$2|E|x = \begin{cases} \int_{\rho_L}^{\rho(x)} \frac{d\rho}{\sqrt{\pi(\rho)}} & 0 \leq x \leq x_+ \\ 2|E|x_+ + \int_{\rho(x)}^{\rho_+} \frac{d\rho}{\sqrt{\pi(\rho)}} & x_+ < x \leq 1 \end{cases} \quad (\text{single-maximum profile}), \quad (\text{S26})$$

where $2|E|x_+ = \int_{\rho_L}^{\rho_+} \frac{d\rho}{\sqrt{\pi(\rho)}}$ defines the position of the maximum. Next, for optimal profiles containing a single minimum $\rho_- = \rho(x_-)$, such that $\pi(\rho_-) = 0$, one can show equivalently

$$2|E|x = \begin{cases} \int_{\rho(x)}^{\rho_L} \frac{d\rho}{\sqrt{\pi(\rho)}} & 0 \leq x \leq x_- \\ 2|E|x_- + \int_{\rho_-}^{\rho(x)} \frac{d\rho}{\sqrt{\pi(\rho)}} & x_- < x \leq 1 \end{cases} \quad (\text{single-minimum profile}), \quad (\text{S27})$$

where now $2|E|x_- = \int_{\rho_-}^{\rho_L} \frac{d\rho}{\sqrt{\pi(\rho)}}$ locates the minimum. Finally, for profiles with a maximum $\rho_+ = \rho(x_+)$ and a minimum $\rho_- = \rho(x_-)$, with $\pi(\rho_+) = 0 = \pi(\rho_-)$, it is easy to see that

$$2|E|x = \begin{cases} \int_{\rho_L}^{\rho(x)} \frac{d\rho}{\sqrt{\pi(\rho)}} & 0 \leq x \leq x_+, \\ 2|E|x_+ + \int_{\rho(x)}^{\rho_+} \frac{d\rho}{\sqrt{\pi(\rho)}} & x_+ < x \leq x_-, \\ 2|E|x_- + \int_{\rho_-}^{\rho(x)} \frac{d\rho}{\sqrt{\pi(\rho)}} & x_- < x \leq 1. \end{cases} \quad (\text{max-min profile}), \quad (\text{S28})$$

with

$$2|E|x_+ = \int_{\rho_L}^{\rho_+} \frac{d\rho}{\sqrt{\pi(\rho)}}, \quad (\text{S29})$$

$$2|E|x_- = 2|E|x_+ + \int_{\rho_-}^{\rho_+} \frac{d\rho}{\sqrt{\pi(\rho)}}. \quad (\text{S30})$$

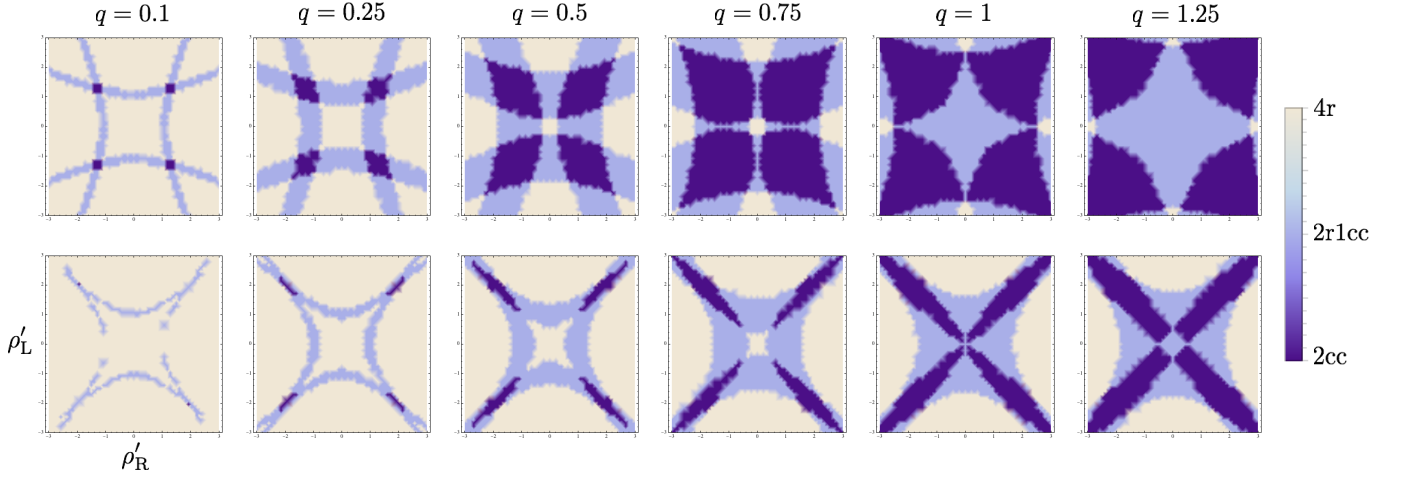


FIG. S2. Density plot of the structure of zeroes of the polynomial $\pi(\rho)$ as a function of the boundary slopes $\rho'_{L,R}(m, q, E) \in [-3, 3]$ for external field $E = 4$ and varying values of the current $q \in [0, 1.25]$. Results for two density gradients are shown, namely $(\rho_L = 0.8, \rho_R = 0.2)$ (symmetric gradient, top row) and $(\rho_L = 0.6, \rho_R = 0.45)$ (asymmetric gradient, bottom row).

Here we implicitly assume that $x_+ < x_-$, i.e. the maximum comes before the minimum. This is a consequence of the choice $\rho_L \geq \rho_R$, which makes the cost of reversing the extrema non-optimal from a variational point of view, see Eq. (S8).

In all cases, the integrals appearing in Eqs. (S25)-(S28) are elliptic integrals of the first kind, whose inverse solution can be written in terms of Jacobi elliptic functions [21], depending on the structure of zeroes of the 4th-order polynomial $\pi(\rho)$. Since this polynomial is always real, its 4 roots can be either two pairs of complex conjugate numbers $(\rho_1, \rho_1^*, \rho_2, \rho_2^* \in \mathbb{C})$, denoted as case 2cc), two real roots accompanied by a single pair of complex conjugate roots $(\rho_1, \rho_2 \in \mathbb{R}, \rho_3, \rho_3^* \in \mathbb{C})$, denoted as case 2r1cc), or 4 different real roots $(\rho_1, \rho_2, \rho_3, \rho_4 \in \mathbb{R})$, denoted as case 4r). Note that all possible combinations do appear in the solution of this variational problem. As an example, Fig. S2 shows density plots for the structure of zeroes of the polynomial $\pi(\rho)$ for a fixed external field $E = 4$ (used below) as a function of the possible boundary slopes of the optimal density field, $\rho'_{L,R}(m, q, E)$, for two different density gradients. We now study each of the cases separately.

A. Two pairs of complex conjugate roots

In this case, due to the absence of real roots, the optimal density profile must be monotonous. This behavior will be dominant for small mass and current fluctuations, i.e. close to the average behavior. If we denote the complex roots as $\rho_1, \rho_1^*, \rho_2, \rho_2^* \in \mathbb{C}$, the polynomial can be written as $\pi(\rho) = (\rho - \rho_1)(\rho - \rho_1^*)(\rho - \rho_2)(\rho - \rho_2^*)$. Defining now $b_i \equiv \text{Re}(\rho_i)$ and $a_i \equiv |\text{Im}(\rho_i)|$, with $i = 1, 2$, and introducing the constants $A^2 \equiv (b_1 - b_2)^2 + (a_1 + a_2)^2$, $B^2 \equiv (b_1 - b_2)^2 + (a_1 - a_2)^2$ and $y_1 \equiv b_1 - a_1 g_1$, with

$$g_1^2 \equiv \frac{4a_1^2 - (A - B)^2}{(A + B)^2 - 4a_1^2}, \quad (\text{S31})$$

we can solve [21] the integral (S25)

$$2|E|x = \int_{y_1}^{\rho_L} \frac{d\rho}{\sqrt{\pi(\rho)}} - \int_{y_1}^{\rho(x)} \frac{d\rho}{\sqrt{\pi(\rho)}} = \frac{2}{A + B} \left[F\left(\varphi(\rho_L), \frac{4AB}{(A + B)^2}\right) - F\left(\varphi(\rho(x)), \frac{4AB}{(A + B)^2}\right) \right], \quad (\text{S32})$$

with

$$\varphi(z) \equiv \tan^{-1} \left(\frac{z - b_1 + a_1 g_1}{a_1 + g_1 b_1 - g_1 z} \right), \quad (\text{S33})$$

and where $F(\varphi(z), k^2)$ is the incomplete elliptic integral of the first kind of amplitude $\varphi(z)$ and modulus k^2 [21]. As originally shown by Abel and Jacobi, this elliptic integral can be inverted [21]. Indeed, if $u \equiv F(\varphi(z), k^2)$, then

$\tan \varphi(z) = \text{tn}(u, k^2)$, where $\text{tn}(u, k^2)$ is the Jacobi tn elliptic function [21]. Applying this inversion formula to

$$F\left(\varphi(\rho(x)), \kappa_\varphi^2\right) = F_\varphi^L - (A+B)|E|x, \quad (\text{S34})$$

where we have defined for simplicity $\kappa_\varphi^2 \equiv 4AB/(A+B)^2$ and $F_\varphi^L \equiv F(\varphi(\rho_L), \kappa_\varphi^2)$, and solving for $\rho(x)$ we find for the case of two complex conjugate roots (2cc)

$$\rho_{2\text{cc}}(x) = \frac{(a_1 + g_1 b_1) \text{tn}\left[F_\varphi^L - (A+B)|E|x, \kappa_\varphi^2\right] + b_1 - a_1 g_1}{1 + g_1 \text{tn}\left[F_\varphi^L - (A+B)|E|x, \kappa_\varphi^2\right]}. \quad (\text{S35})$$

B. Two real roots, one pair of complex conjugate roots

We denote the real roots as $\rho_1, \rho_2 \in \mathbb{R}$, while the pair of complex conjugate roots is $\rho_3, \rho_3^* \in \mathbb{C}$. We further assume without loss of generality that $\rho_1 < \rho_2$. Due to the presence of two real roots, the number of possibilities to study increases considerably. In particular, the two real roots can be either:

(i) $\rho_1, \rho_2 \geq \rho_L$.

In this case the density profile can be monotonous (i1) or it may have a single maximum at ρ_1 (i2). The polynomial $\pi(\rho)$ can be now written in the region of interest as $\pi(\rho) = (\rho_1 - \rho)(\rho_2 - \rho)(\rho - \rho_3)(\rho - \rho_3^*)$. Defining now $b_3 \equiv \text{Re}(\rho_3)$ and $a_3 \equiv |\text{Im}(\rho_3)|$, and introducing the constants $A^2 \equiv (\rho_1 - b_3)^2 + a_3^2$ and $B^2 \equiv (\rho_2 - b_3)^2 + a_3^2$, we have for the case (i1) of monotonous profiles, see Eq. (S25), that

$$2|E|x = \int_{\rho(x)}^{\rho_1} \frac{d\rho}{\sqrt{\pi(\rho)}} - \int_{\rho_L}^{\rho_1} \frac{d\rho}{\sqrt{\pi(\rho)}} = \frac{1}{\sqrt{AB}} \left[F\left(\gamma(\rho(x)), \kappa_\gamma^2\right) - F_\gamma^L \right], \quad (\text{S36})$$

where $F(\gamma(z), \kappa_\gamma^2)$ is the incomplete elliptic integral of the first kind of amplitude $\gamma(z)$ and modulus κ_γ^2 [21]. We have further defined the amplitude function

$$\gamma(z) \equiv \cos^{-1} \left(\frac{(A-B)z + \rho_1 B - \rho_2 A}{(A+B)z - \rho_1 B - \rho_2 A} \right)^{s_+}, \quad (\text{S37})$$

as well as the modulus

$$\kappa_\gamma^2 \equiv s_+ \frac{(A + s_+ B)^2 - (\rho_1 - \rho_2)^2}{4AB}, \quad (\text{S38})$$

and the constant $F_\gamma^L \equiv F(\gamma(\rho_L), \kappa_\gamma^2)$, where we introduce for latter convenience the sign function $s_+ \equiv (-1)^{n_+}$, with n_+ the number of real roots larger or equal than ρ_L [note that for the current case (i) $s_+ = +1$ as $n_+ = 2$]. As before, if $u \equiv F(\gamma(z), k^2)$, then $\cos \gamma(z) = \text{cn}(u, k^2)$, where $\text{cn}(u, k^2)$ is the Jacobi cosine elliptic function [21]. Applying this inversion formula to

$$F\left(\gamma(\rho(x)), \kappa_\gamma^2\right) = F_\gamma^L + 2|E|\sqrt{AB}x \quad (\text{S39})$$

and solving for $\rho(x)$ we obtain for the case of two real (2r) and one pair of complex conjugate roots (1cc) in the case (i1) of monotonous profiles

$$\rho_{2\text{r}1\text{cc}}^{(\text{i1})}(x) = \frac{(\rho_2 A - \rho_1 B) - (\rho_1 B + \rho_2 A) \text{cn}\left[F_\gamma^L + 2|E|\sqrt{AB}x, \kappa_\gamma^2\right]}{(A-B) - (A+B) \text{cn}\left[F_\gamma^L + 2|E|\sqrt{AB}x, \kappa_\gamma^2\right]}. \quad (\text{S40})$$

Next we consider a profile with a single maximum (i2). In this case, see Eq. (S26),

$$2|E|x = \begin{cases} \int_{\rho_L}^{\rho_1} \frac{d\rho}{\sqrt{\pi(\rho)}} - \int_{\rho(x)}^{\rho_1} \frac{d\rho}{\sqrt{\pi(\rho)}} = \frac{1}{\sqrt{AB}} \left[F_\gamma^L - F\left(\gamma(\rho(x)), \kappa_\gamma^2\right) \right] & 0 \leq x \leq x_+ \\ \int_{\rho_L}^{\rho_1} \frac{d\rho}{\sqrt{\pi(\rho)}} + \int_{\rho(x)}^{\rho_1} \frac{d\rho}{\sqrt{\pi(\rho)}} = \frac{1}{\sqrt{AB}} \left[F_\gamma^L + F\left(\gamma(\rho(x)), \kappa_\gamma^2\right) \right] & x_+ < x \leq 1 \end{cases} \quad (\text{S41})$$

where $2|E|x_+ = F_\gamma^L/\sqrt{AB}$. We therefore have

$$F\left(\gamma(\rho(x)), \kappa_\gamma^2\right) = 2|E|\sqrt{AB}|x_+ - x| = |F_\gamma^L - 2|E|\sqrt{AB}x|, \quad (\text{S42})$$

which can be inverted to obtain

$$\rho_{2r1cc}^{(i2)}(x) = \frac{(\rho_2 A - \rho_1 B) - (\rho_1 B + \rho_2 A) \operatorname{cn}\left[|F_\gamma^L - 2|E|\sqrt{AB}x|, \kappa_\gamma^2\right]}{(A - B) - (A + B) \operatorname{cn}\left[|F_\gamma^L - 2|E|\sqrt{AB}x|, \kappa_\gamma^2\right]}. \quad (\text{S43})$$

The solution for both the monotonous (i1) and the single-maximum (i2) cases when $\rho_1, \rho_2 \geq \rho_L$ can be now unified by introducing the slope of the optimal profile at the left boundary and its sign. In particular, defining the boundary slopes $\rho'_L \equiv \rho'(0)$ and $\rho'_R \equiv \rho'(1)$, and introducing their sign $s_{L,R} \equiv \operatorname{sign}(\rho'_{L,R})$, it's clear that the monotonous profile for $\rho_L \geq \rho_R$ corresponds to $s_L = -1$ while the single-maximum case corresponds to $s_L = +1$, and hence

$$\rho_{2r1cc}^{(i)}(x) = \frac{(\rho_2 A - \rho_1 B) - (\rho_1 B + \rho_2 A) \operatorname{cn}\left[|F_\gamma^L - 2s_L|E|\sqrt{AB}x|, \kappa_\gamma^2\right]}{(A - B) - (A + B) \operatorname{cn}\left[|F_\gamma^L - 2s_L|E|\sqrt{AB}x|, \kappa_\gamma^2\right]} \quad (\text{S44})$$

represents both solutions for the case (i) $\rho_1, \rho_2 \geq \rho_L$.

(ii) $\rho_1, \rho_2 \leq \rho_R$.

In this case the density profile can be monotonous (ii1) or it may have a single minimum (ii2) at ρ_2 (since in our notation $\rho_1 < \rho_2$). Note that, as in case (i) above, the roots sign function is again $s_+ = +1$ since $n_+ = 0$ here. We proceed now as above and write the polynomial $\pi(\rho)$ in the interesting regime as $\pi(\rho) = (\rho - \rho_1)(\rho - \rho_2)(\rho - \rho_3)(\rho - \rho_3^*)$. As before, for the case of monotonous profiles we may write

$$\begin{aligned} 2|E|x &= \int_{\rho_2}^{\rho_L} \frac{d\rho}{\sqrt{\pi(\rho)}} - \int_{\rho_2}^{\rho(x)} \frac{d\rho}{\sqrt{\pi(\rho)}} = \frac{1}{\sqrt{AB}} \left[F\left(\pi - \gamma(\rho_L), \kappa_\gamma^2\right) - F\left(\pi - \gamma(\rho(x)), \kappa_\gamma^2\right) \right] \\ &= \frac{1}{\sqrt{AB}} \left[F\left(\gamma(\rho(x)), \kappa_\gamma^2\right) - F_\gamma^L \right], \end{aligned} \quad (\text{S45})$$

where we have used that $\cos^{-1}(-z) = \pi - \cos^{-1}(z)$ and $F(\pi - \gamma, k^2) = 2K(k^2) - F(\gamma, k^2)$, with $K(k^2) = F(\pi/2, k^2)$ the complete elliptic integral of the first kind. The previous equation once inverted in terms of Jacobi cosine elliptic functions and solved for $\rho(x)$ yields the same Eq. (S40) as in case (i1) above, i.e. $\rho_{2r1cc}^{(ii1)}(x) = \rho_{2r1cc}^{(i1)}(x)$.

In a similar way, when the profile has a single-minimum we have [21]

$$2|E|x = \begin{cases} \int_{\rho_2}^{\rho_L} \frac{d\rho}{\sqrt{\pi(\rho)}} - \int_{\rho_2}^{\rho(x)} \frac{d\rho}{\sqrt{\pi(\rho)}} = \frac{1}{\sqrt{AB}} \left[F\left(\pi - \gamma(\rho_L), \kappa_\gamma^2\right) - F\left(\pi - \gamma(\rho(x)), \kappa_\gamma^2\right) \right] & 0 \leq x \leq x_- \\ \int_{\rho_2}^{\rho_L} \frac{d\rho}{\sqrt{\pi(\rho)}} + \int_{\rho_2}^{\rho(x)} \frac{d\rho}{\sqrt{\pi(\rho)}} = \frac{1}{\sqrt{AB}} \left[F\left(\pi - \gamma(\rho_L), \kappa_\gamma^2\right) + F\left(\pi - \gamma(\rho(x)), \kappa_\gamma^2\right) \right] & x_- < x \leq 1 \end{cases} \quad (\text{S46})$$

or equivalently

$$2|E|x = \begin{cases} \frac{1}{\sqrt{AB}} \left[F\left(\gamma(\rho(x)), \kappa_\gamma^2\right) - F_\gamma^L \right] & 0 \leq x \leq x_- \\ \frac{1}{\sqrt{AB}} \left[4K(k^2) - F\left(\gamma(\rho(x)), \kappa_\gamma^2\right) - F_\gamma^L \right] & x_- < x \leq 1 \end{cases} \quad (\text{S47})$$

Solving for $F\left(\gamma(\rho(x)), \kappa_\gamma^2\right)$ in the previous piece-wise equation, applying the inversion formula and noting that $\text{cn}(u, k^2)$ is even in u and periodic with period $4K(k^2)$, i.e. $\text{cn}(u + 4K(k^2), k^2) = \text{cn}(u) = \text{cn}(-u)$, see Ref. [21], we thus find after solving for the density profile

$$\rho_{2r1cc}^{(ii2)}(x) = \frac{(\rho_2 A - \rho_1 B) - (\rho_1 B + \rho_2 A) \text{cn}\left[F_\gamma^L + 2|E|\sqrt{AB}x, \kappa_\gamma^2\right]}{(A - B) - (A + B) \text{cn}\left[F_\gamma^L + 2|E|\sqrt{AB}x, \kappa_\gamma^2\right]} = \rho_{2r1cc}^{(ii1)}(x) = \rho_{2r1cc}^{(i1)}(x), \quad (\text{S48})$$

so the general formula (S44) for case (i) is also valid for case (ii) [note that in the latter case the sign of the profile slope at the left boundary is $s_L = -1$].

(iii) $\rho_1 \leq \rho_R, \rho_2 \geq \rho_L$.

In this case the density profile can be monotonous (iii1) or it may a single maximum (iii2), a single minimum (iii3), or a maximum and a minimum (iii4). In all cases the roots sign function is now $s_+ = -1$ since $n_+ = 1$. The polynomial $\pi(\rho)$ can be decomposed as $\pi(\rho) = (\rho - \rho_1)(\rho_2 - \rho)(\rho - \rho_3)(\rho - \rho_3^*)$, and for the case (iii1) of monotonous profiles –see Eq. (S25)– we find

$$2|E|x = \int_{\rho_1}^{\rho_L} \frac{d\rho}{\sqrt{\pi(\rho)}} - \int_{\rho_1}^{\rho(x)} \frac{d\rho}{\sqrt{\pi(\rho)}} = \frac{1}{\sqrt{AB}} \left[F_\gamma^L - F\left(\gamma(\rho(x)), \kappa_\gamma^2\right) \right], \quad (\text{S49})$$

and therefore

$$\rho_{2r1cc}^{(iii1)}(x) = \frac{(\rho_2 A - \rho_1 B) - (\rho_1 B + \rho_2 A) \left(\text{cn}\left[F_\gamma^L - 2|E|\sqrt{AB}x, \kappa_\gamma^2\right] \right)^{-1}}{(A - B) - (A + B) \left(\text{cn}\left[F_\gamma^L - 2|E|\sqrt{AB}x, \kappa_\gamma^2\right] \right)^{-1}}. \quad (\text{S50})$$

When a single maximum is presents, case (iii2), we have

$$2|E|x = \begin{cases} \int_{\rho_1}^{\rho(x)} \frac{d\rho}{\sqrt{\pi(\rho)}} - \int_{\rho_1}^{\rho_L} \frac{d\rho}{\sqrt{\pi(\rho)}} = \frac{1}{\sqrt{AB}} \left[F\left(\gamma(\rho(x)), \kappa_\gamma^2\right) - F_\gamma^L \right] & 0 \leq x \leq x_+ \\ 2 \int_{\rho_1}^{\rho_2} \frac{d\rho}{\sqrt{\pi(\rho)}} - \int_{\rho_1}^{\rho_L} \frac{d\rho}{\sqrt{\pi(\rho)}} - \int_{\rho_1}^{\rho(x)} \frac{d\rho}{\sqrt{\pi(\rho)}} = \frac{1}{\sqrt{AB}} \left[4K(\kappa_\gamma^2) - F_\gamma^L - F\left(\gamma(\rho(x)), \kappa_\gamma^2\right) \right] & x_+ < x \leq 1 \end{cases} \quad (\text{S51})$$

where the maximum location is given now by $2|E|\sqrt{AB}x_+ = 4K(\kappa_\gamma^2) - F_\gamma^L/\sqrt{AB}$. Solving for $F\left(\gamma(\rho(x)), \kappa_\gamma^2\right)$, applying the inversion formula and recalling that $\text{cn}(u + 4K(k^2), k^2) = \text{cn}(u) = \text{cn}(-u)$, we thus find after solving for the density profile

$$\rho_{2r1cc}^{(iii2)}(x) = \frac{(\rho_2 A - \rho_1 B) - (\rho_1 B + \rho_2 A) \left(\text{cn}\left[F_\gamma^L + 2|E|\sqrt{AB}x, \kappa_\gamma^2\right] \right)^{-1}}{(A - B) - (A + B) \left(\text{cn}\left[F_\gamma^L + 2|E|\sqrt{AB}x, \kappa_\gamma^2\right] \right)^{-1}}. \quad (\text{S52})$$

For the single-minimum case (iii3) we have

$$2|E|x = \begin{cases} \int_{\rho_1}^{\rho_L} \frac{d\rho}{\sqrt{\pi(\rho)}} - \int_{\rho_1}^{\rho(x)} \frac{d\rho}{\sqrt{\pi(\rho)}} = \frac{1}{\sqrt{AB}} \left[F_\gamma^L - F\left(\gamma(\rho(x)), \kappa_\gamma^2\right) \right] & 0 \leq x \leq x_- \\ \int_{\rho_1}^{\rho_L} \frac{d\rho}{\sqrt{\pi(\rho)}} + \int_{\rho_1}^{\rho(x)} \frac{d\rho}{\sqrt{\pi(\rho)}} = \frac{1}{\sqrt{AB}} \left[F_\gamma^L + F\left(\gamma(\rho(x)), \kappa_\gamma^2\right) \right] & x_- < x \leq 1 \end{cases} \quad (\text{S53})$$

with $x_- = F_\gamma^L/(2|E|\sqrt{AB})$, and therefore

$$\rho_{2r1cc}^{(iii3)}(x) = \frac{(\rho_2 A - \rho_1 B) - (\rho_1 B + \rho_2 A) \left(\text{cn}\left[|F_\gamma^L - 2|E|\sqrt{AB}x|, \kappa_\gamma^2\right] \right)^{-1}}{(A - B) - (A + B) \left(\text{cn}\left[|F_\gamma^L - 2|E|\sqrt{AB}x|, \kappa_\gamma^2\right] \right)^{-1}}. \quad (\text{S54})$$

Finally, for the case (iii4) with a maximum and a minimum, we can write

$$2|E|x = \begin{cases} \int_{\rho_1}^{\rho(x)} \frac{d\rho}{\sqrt{\pi(\rho)}} - \int_{\rho_1}^{\rho_L} \frac{d\rho}{\sqrt{\pi(\rho)}} = \frac{1}{\sqrt{AB}} \left[F\left(\gamma(\rho(x)), \kappa_\gamma^2\right) - F_\gamma^L \right] & 0 \leq x \leq x_+ \\ 2 \int_{\rho_1}^{\rho_2} \frac{d\rho}{\sqrt{\pi(\rho)}} - \int_{\rho_1}^{\rho_L} \frac{d\rho}{\sqrt{\pi(\rho)}} - \int_{\rho_1}^{\rho(x)} \frac{d\rho}{\sqrt{\pi(\rho)}} = \frac{1}{\sqrt{AB}} \left[4K(\kappa_\gamma^2) - F_\gamma^L - F\left(\gamma(\rho(x)), \kappa_\gamma^2\right) \right] & x_+ < x \leq x_- \\ 2 \int_{\rho_1}^{\rho_2} \frac{d\rho}{\sqrt{\pi(\rho)}} - \int_{\rho_1}^{\rho_L} \frac{d\rho}{\sqrt{\pi(\rho)}} + \int_{\rho_1}^{\rho(x)} \frac{d\rho}{\sqrt{\pi(\rho)}} = \frac{1}{\sqrt{AB}} \left[4K(\kappa_\gamma^2) - F_\gamma^L + F\left(\gamma(\rho(x)), \kappa_\gamma^2\right) \right] & x_- < x \leq 1 \end{cases} \quad (\text{S55})$$

or equivalently

$$F\left(\gamma(\rho(x)), \kappa_\gamma^2\right) = \begin{cases} F_\gamma^L + 2|E|\sqrt{AB}x & 0 \leq x \leq x_+ \\ 4K(\kappa_\gamma^2) - (F_\gamma^L + 2|E|\sqrt{AB}x) & x_+ < x \leq x_- \\ (F_\gamma^L + 2|E|\sqrt{AB}x) - 4K(\kappa_\gamma^2) & x_- < x \leq 1 \end{cases} \quad (\text{S56})$$

where $x_+ = (2K(\kappa_\gamma^2) - F_\gamma^L)/(2|E|\sqrt{AB})$ and $x_- = (4K(\kappa_\gamma^2) - F_\gamma^L)/(2|E|\sqrt{AB})$. Inverting the previous piecewise equation, taking into account the periodicity of the Jacobi cosine elliptic function $\text{cn}(u, k^2)$, and solving for the density we thus find

$$\rho_{2r1cc}^{(iii4)}(x) = \frac{(\rho_2 A - \rho_1 B) - (\rho_1 B + \rho_2 A) \left(\text{cn} \left[F_\gamma^L + 2|E|\sqrt{AB}x, \kappa_\gamma^2 \right] \right)^{-1}}{(A - B) - (A + B) \left(\text{cn} \left[F_\gamma^L + 2|E|\sqrt{AB}x, \kappa_\gamma^2 \right] \right)^{-1}}. \quad (\text{S57})$$

It is now clear that the four different options for case (iii) with $\rho_1 \leq \rho_R$, $\rho_2 \geq \rho_L$ can be unified into a single expression using the sign of the left boundary slope s_L , i.e. with the argument of the cn function written as $|F_\gamma^L + 2s_L|E|\sqrt{AB}x|$. Moreover, using also the roots sign function s_+ defined above, we may write the general solution for the case of two real roots and one pair of complex conjugate roots for $\pi(\rho)$ in a compact form

$$\rho_{2r1cc}(x) = \frac{(\rho_2 A - \rho_1 B) - (\rho_1 B + \rho_2 A) \left(\text{cn} \left[|F_\gamma^L - 2s_L s_+|E|\sqrt{AB}x|, \kappa_\gamma^2 \right] \right)^{s_+}}{(A - B) - (A + B) \left(\text{cn} \left[|F_\gamma^L - 2s_L s_+|E|\sqrt{AB}x|, \kappa_\gamma^2 \right] \right)^{s_+}}. \quad (\text{S58})$$

C. Four real roots

We denote the real roots as $\rho_1 < \rho_2 < \rho_3 < \rho_4 \in \mathbb{R}$, where the label ordering is arbitrary. As in Section A.3.2 above, we should now explore all possible orderings of these 4 real roots with respect to the boundary densities $\rho_L \geq \rho_R$. However, one can check numerically that the only ordering appearing in all cases of interest is that of two real roots above ρ_L and two real roots below ρ_R , i.e. $\rho_1 < \rho_2 < \rho_R \leq \rho_L < \rho_3 < \rho_4$, in which case the polynomial can be written in the regime of interest as $\pi(\rho) = (\rho_1 - \rho)(\rho_2 - \rho)(\rho - \rho_3)(\rho - \rho_4)$. Due to the presence of two real roots bracketing the boundary densities, the resulting density profile can be monotonous (iv1), or it may have a single maximum (iv2), a single minimum (iv3), or a maximum and a minimum (iv4). Defining now the constant $g_\phi \equiv \sqrt{(\rho_4 - \rho_2)(\rho_3 - \rho_1)}$ and the amplitude function

$$\phi(z) \equiv \sin^{-1} \sqrt{\frac{(\rho_4 - \rho_2)(\rho_3 - z)}{(\rho_3 - \rho_2)(\rho_4 - z)}}, \quad (\text{S59})$$

together with the modulus

$$\kappa_\phi^2 \equiv \frac{(\rho_3 - \rho_2)(\rho_4 - \rho_1)}{(\rho_4 - \rho_2)(\rho_3 - \rho_1)}, \quad (\text{S60})$$

we find for the monotonous case (iv1) that

$$2|E|x = \int_{\rho(x)}^{\rho_3} \frac{d\rho}{\sqrt{\pi(\rho)}} - \int_{\rho_L}^{\rho_3} \frac{d\rho}{\sqrt{\pi(\rho)}} = \frac{2}{g_\phi} \left[F\left(\phi(\rho(x)), \kappa_\phi^2\right) - F_\phi^L \right] \quad (\text{S61})$$

where $F(\phi(z), \kappa_\phi^2)$ is the incomplete elliptic integral of the first kind with amplitude $\phi(z)$ and modulus κ_ϕ^2 , see Eqs. (S59) and (S60), and $F_\phi^L \equiv F(\phi(\rho_L), \kappa_\phi^2)$. By noting that if $u \equiv F(\phi(z), k^2)$, then $\sin \gamma(z) = \text{sn}(u, k^2)$, where $\text{sn}(u, k^2)$ is the Jacobi sine elliptic function [21], we thus find

$$\frac{(\rho_4 - \rho_2)(\rho_3 - \rho(x))}{(\rho_3 - \rho_2)(\rho_4 - \rho(x))} = \text{sn}^2\left(g_\phi|E|x + F_\phi^L, \kappa_\phi^2\right), \quad (\text{S62})$$

which can be solved for $\rho(x)$ to yield

$$\rho_{4r}^{(\text{iv1})}(x) = \rho_4 \frac{A_\phi \text{sn}^2\left(g_\phi|E|x + F_\phi^L, \kappa_\phi^2\right) - \rho_3/\rho_4}{A_\phi \text{sn}^2\left(g_\phi|E|x + F_\phi^L, \kappa_\phi^2\right) - 1}, \quad (\text{S63})$$

where $A_\phi \equiv (\rho_3 - \rho_2)/(\rho_4 - \rho_2)$ is another constant. For the case (iv2) of profiles exhibiting a single maximum, proceeding as in previous examples one simply obtains

$$F\left(\phi(\rho(x)), \kappa_\phi^2\right) = \begin{cases} F_\phi^L - g_\phi|E|x & 0 \leq x \leq x_+ \\ -(F_\phi^L - g_\phi|E|x) & x_+ < x \leq 1 \end{cases} \quad (\text{S64})$$

where the maximum location is defined by $g_\phi|E|x_+ = F_\phi^L$. Inverting the previous equation and solving for the density field we hence find

$$\rho_{4r}^{(\text{iv2})}(x) = \rho_4 \frac{A_\phi \text{sn}^2\left(|F_\phi^L - g_\phi|E|x|, \kappa_\phi^2\right) - \rho_3/\rho_4}{A_\phi \text{sn}^2\left(|F_\phi^L - g_\phi|E|x|, \kappa_\phi^2\right) - 1}. \quad (\text{S65})$$

For the single minimum case (iv3), we have

$$2|E|x = \begin{cases} \int_{\rho(x)}^{\rho_3} \frac{d\rho}{\sqrt{\pi(\rho)}} - \int_{\rho_L}^{\rho_3} \frac{d\rho}{\sqrt{\pi(\rho)}} = \frac{2}{g_\phi} \left[F\left(\phi(\rho(x)), \kappa_\phi^2\right) - F_\phi^L \right] & 0 \leq x \leq x_- \\ 2 \int_{\rho_2}^{\rho_3} \frac{d\rho}{\sqrt{\pi(\rho)}} - \int_{\rho_L}^{\rho_3} \frac{d\rho}{\sqrt{\pi(\rho)}} - \int_{\rho(x)}^{\rho_3} \frac{d\rho}{\sqrt{\pi(\rho)}} = \frac{2}{g_\phi} \left[2K(\kappa_\phi^2) - F_\phi^L - F\left(\phi(\rho(x)), \kappa_\phi^2\right) \right] & x_- < x \leq 1 \end{cases} \quad (\text{S66})$$

or equivalently

$$F\left(\phi(\rho(x)), \kappa_\phi^2\right) = \begin{cases} F_\phi^L + g_\phi|E|x & 0 \leq x \leq x_- \\ 2K(\kappa_\phi^2) - (F_\phi^L + g_\phi|E|x) & x_- < x \leq 1 \end{cases} \quad (\text{S67})$$

This expression can be easily inverted by noting [21] that $\text{sn}(u + 2K(k^2), k^2) = -\text{sn}(u, k^2) = \text{sn}(-u, k^2)$, and solving for the density profile we thus obtain $\rho_{4r}^{(\text{iv3})}(x) = \rho_{4r}^{(\text{iv1})}(x)$, i.e. the same expression as in case (iv1) above, see Eq. (S63). Finally, for the case (iv4) of a profile with a maximum and a minimum, we have

$$2|E|x = \begin{cases} \int_{\rho_L}^{\rho_3} \frac{d\rho}{\sqrt{\pi(\rho)}} - \int_{\rho(x)}^{\rho_3} \frac{d\rho}{\sqrt{\pi(\rho)}} = \frac{2}{g_\phi} \left[F_\phi^L - F\left(\phi(\rho(x)), \kappa_\phi^2\right) \right] & 0 \leq x \leq x_+ \\ \int_{\rho_L}^{\rho_3} \frac{d\rho}{\sqrt{\pi(\rho)}} + \int_{\rho(x)}^{\rho_3} \frac{d\rho}{\sqrt{\pi(\rho)}} = \frac{2}{g_\phi} \left[F_\phi^L + F\left(\phi(\rho(x)), \kappa_\phi^2\right) \right] & x_+ < x \leq x_- \\ 2 \int_{\rho_2}^{\rho_3} \frac{d\rho}{\sqrt{\pi(\rho)}} + \int_{\rho_L}^{\rho_3} \frac{d\rho}{\sqrt{\pi(\rho)}} - \int_{\rho(x)}^{\rho_3} \frac{d\rho}{\sqrt{\pi(\rho)}} = \frac{2}{g_\phi} \left[2K(\kappa_\phi^2) + F_\phi^L - F\left(\phi(\rho(x)), \kappa_\phi^2\right) \right] & x_- < x \leq 1 \end{cases} \quad (\text{S68})$$

or equivalently

$$F\left(\phi(\rho(x)), \kappa_\phi^2\right) = \begin{cases} F_\phi^L - g_\phi|E|x & 0 \leq x \leq x_+ \\ -(F_\phi^L - g_\phi|E|x) & x_+ < x \leq x_- \\ 2K(\kappa_\phi^2) + F_\phi^L - g_\phi|E|x & x_- < x \leq 1 \end{cases} \quad (\text{S69})$$

with $g_\phi|E|x_+ = F_\phi^L$ and $g_\phi|E|x_- = F_\phi^L + K(\kappa_\phi^2)$. Using again the periodicity of the Jacobi elliptic sn function, and solving for the density profile, it is easy to find that $\rho_{4r}^{(iv4)}(x) = \rho_{4r}^{(iv2)}(x)$, i.e. the same expression as in case (iv2) above, see Eq. (S65). Moreover, all expressions for cases (iv1)–(iv4) (when $\pi(\rho)$ has four real roots) can be unified into a single formula by making use again of the left boundary slope sign function s_L , i.e. the sign of the slope of the density field $\rho(x)$ at $x = 0$. The result is

$$\rho_{4r}(x) = \rho_4 \frac{A_\phi \operatorname{sn}^2\left(|F_\phi^L - s_L g_\phi|E|x|, \kappa_\phi^2\right) - \rho_3/\rho_4}{A_\phi \operatorname{sn}^2\left(|F_\phi^L - s_L g_\phi|E|x|, \kappa_\phi^2\right) - 1}. \quad (\text{S70})$$

In summary, the general solution for the optimal density field associated to a joint mass and current fluctuation in the 1d weakly asymmetric simple exclusion process in contact with boundary reservoirs at densities $\rho_L \geq \rho_R$ and subject to an external driving field E can be written as

$$\rho(x) = \begin{cases} \frac{(a_1 + g_1 b_1) \operatorname{tn}\left[F_\phi^L - (A + B)|E|x, \kappa_\phi^2\right] + b_1 - a_1 g_1}{1 + g_1 \operatorname{tn}\left[F_\phi^L - (A + B)|E|x, \kappa_\phi^2\right]} & (2cc) \\ \frac{(\rho_2 A - \rho_1 B) - (\rho_1 B + \rho_2 A) \left(\operatorname{cn}\left[|F_\gamma^L - 2s_L s_+|E|\sqrt{AB}x|, \kappa_\gamma^2\right]\right)^{s_+}}{(A - B) - (A + B) \left(\operatorname{cn}\left[|F_\gamma^L - 2s_L s_+|E|\sqrt{AB}x|, \kappa_\gamma^2\right]\right)^{s_+}} & (2r1cc) \\ \rho_4 \frac{A_\phi \operatorname{sn}^2\left(|F_\phi^L - s_L g_\phi|E|x|, \kappa_\phi^2\right) - \rho_3/\rho_4}{A_\phi \operatorname{sn}^2\left(|F_\phi^L - s_L g_\phi|E|x|, \kappa_\phi^2\right) - 1} & (4r) \end{cases} \quad (\text{S71})$$

where the relevant constants in each case are defined above.

Using this result, it is now possible to study analytically the dynamical phase transition described in the main text for arbitrary boundary gradient (symmetric or asymmetric), well beyond the perturbative nonequilibrium linear regime. In particular, for PH-symmetric boundaries ($\rho_R = 1 - \rho_L$), the conditional mass-current LDF $G(m|q) \equiv G(m, q) - G(q)$ exhibits a peculiar change of behavior at a critical current $|q_c|$, see Figs. S3.a-b: while for $|q| > |q_c|$ the LDF $G(m|q)$ displays a single minimum at $m_q = 1/2$, with an associated PH-symmetric optimal profile (top insets in Figs. S3.a-b), for $|q| < |q_c|$ two equivalent minima m_q^\pm appear in $G(m|q)$, each one associated with a PH-symmetry-broken optimal profile $\rho_q^\pm(x)$, see bottom insets in Figs. S3.a-b, such that $\rho_q^\pm(x) \rightarrow 1 - \rho_q^\mp(1 - x)$. The emergence of this non-convex regime in $G(m|q)$ signals a 2nd-order DPT to a PH-symmetry-broken dynamical phase. Note that this happens both for equal boundary densities ($\rho_R = 0.5 = \rho_L$, Fig. S3.a) and for large but symmetric boundary gradients ($\rho_L = 0.8, \rho_R = 0.2$, Fig. S3.b). On the other hand, for PH-asymmetric boundaries ($\rho_R \neq 1 - \rho_L$, as e.g. $\rho_L = 0.6, \rho_R = 0.45$, see Fig. S3.c), the governing action (S4) is no longer PH-symmetric: the asymmetry favors one of the mass branches and the associated $G(m|q)$ displays a single *global* minimum $\forall q$, see Fig. S3.c, and an unique optimal profile. Still, $G(m|q)$ becomes non-convex for low enough currents, and for weak gradient asymmetry, as is the case for $\rho_L = 0.6, \rho_R = 0.45$ shown in Fig. S3.c, metastable-like local minima in $G(m|q)$ may appear.

The mass m_q where the minima of $G(m|q)$ appear for a fixed q is evaluated by demanding $\frac{dG(m|q)}{dm} = \frac{dG(m, q)}{dm} = 0$. The m -slope of the LDF $G(m, q)$ at a given (m, q) -point is simply given by the Lagrange multiplier $\lambda(m, q)$ used to impose the mass constraint, so

$$\left. \frac{dG(m, q)}{dm} \right|_{m_q} = \lambda(m_q, q) = 0 \quad \Rightarrow \quad \Lambda_L(m_q, q, E) = \Lambda_R(m, q, E), \quad (\text{S72})$$

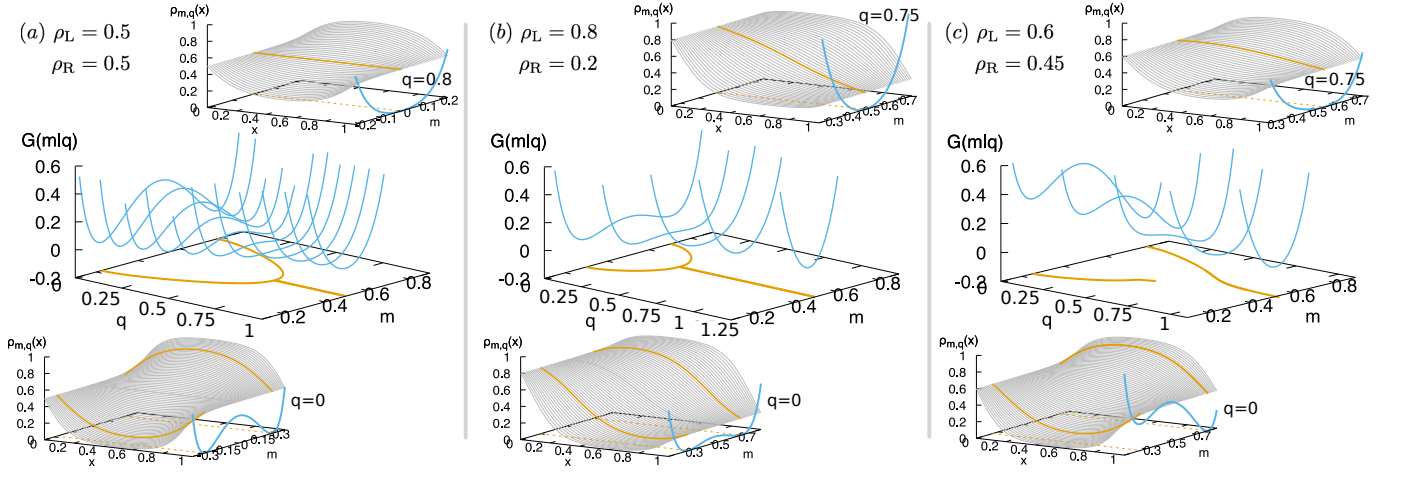


FIG. S3. Middle row: Conditional LDF $G(m|q) = G(m, q) - G(q)$ as a function of the mass m for different currents q for three different boundary drivings, namely (a) $\rho_L = 0.5, \rho_R = 0.5$ (symmetric driving), (b) $\rho_L = 0.8, \rho_R = 0.2$ (symmetric driving), and (c) $\rho_L = 0.6, \rho_R = 0.45$ (asymmetric driving). The lines projected in the $m - q$ plane correspond to the local minima of the LDF $G(m|q)$, which define the mass m_q associated to a current fluctuation q . In the symmetry-broken regime this defines the low- and high-mass branches m_q^\pm . Bottom row: optimal density profiles $\rho_{m,q}(x)$ obtained for $q = 0$ and the three different boundary drivings. The thick lines are the optimal profiles associated to the local minima m_q^\pm of $G(m|q)$. For completeness the associated $G(m|q)$ is also shown. Top row: optimal density profiles in each case, for a current in the PH-symmetric region, $|q| > q_c$.

where we have used the formula which relates the Lagrange multiplier $\lambda(m, q)$ with the boundary slopes $\rho'_{L,R}(m, q, E)$ of the optimal density profile, see Eq. (S22) in §III above, with the definition

$$\Lambda_{L,R}(m, q, E) \equiv \frac{\frac{1}{4}(\rho'_{L,R})^2(m, q, E) - q^2 - E^2 \rho_{L,R}^2(1 - \rho_{L,R})^2}{2\rho_{L,R}(1 - \rho_{L,R})}. \quad (\text{S73})$$

In this way, defining $\sigma_{L,R} \equiv \rho_{L,R}(1 - \rho_{L,R})$, the equation for the mass minima m_q for a fixed q is

$$\frac{1}{4\sigma_L}(\rho'_L)^2(m_q, q, E) - \frac{1}{4\sigma_R}(\rho'_R)^2(m_q, q, E) = q^2 \left(\frac{1}{\sigma_L} - \frac{1}{\sigma_R} \right) + E^2(\sigma_L - \sigma_R). \quad (\text{S74})$$

The critical current q_c can be evaluated as well by demanding that

$$\left. \frac{dG(m, q)}{dm} \right|_{m_{q_c}, q_c} = 0 = \left. \frac{d^2G(m, q)}{dm^2} \right|_{m_{q_c}, q_c}, \quad (\text{S75})$$

which leads to the following pair of equations

$$\frac{1}{4\sigma_L}(\rho'_L)^2(m_{q_c}, q_c, E) - \frac{1}{4\sigma_R}(\rho'_R)^2(m_{q_c}, q_c, E) = q_c^2 \left(\frac{1}{\sigma_L} - \frac{1}{\sigma_R} \right) + E^2(\sigma_L - \sigma_R), \quad (\text{S76})$$

$$\left. \frac{\rho'_L(m, q, E)}{\sigma_L} \frac{d\rho'_L(m, q, E)}{dm} \right|_{m_{q_c}, q_c} = \left. \frac{\rho'_R(m, q, E)}{\sigma_R} \frac{d\rho'_R(m, q, E)}{dm} \right|_{m_{q_c}, q_c}. \quad (\text{S77})$$

Note that these equations for m_q and for q_c must be solved numerically due to the nonlinear character of the problem.

IV. INSTANTON SOLUTION, MAXWELL-LIKE CONSTRUCTION AND VIOLATION OF ADDITIVITY PRINCIPLE

In this section we build a time-dependent, instanton-like solution for the optimal density and current fields responsible of a joint fluctuation of the empirical current and mass. We further show that this solution improves the additivity principle prediction (i.e. yields a better minimizer of the MFT action) in the regime where the joint current-mass LDF becomes non-convex. This result demonstrates that time-dependent solutions of the MFT problem in open systems exist and dominate fluctuation behavior in dynamical coexistence regimes emerging at DPTs.

We start from the general expression derived above for the joint mass-current LDF, see Eq. (S7),

$$G(m, q) = \lim_{\tau \rightarrow \infty} \frac{1}{\tau} \min_{\{\rho, j\}_0^\tau} \int_0^\tau dt \int_0^1 dx \frac{[j + D(\rho)\partial_x \rho - E\sigma(\rho)]^2}{2\sigma(\rho)}, \quad (\text{S78})$$

with the fields $\rho(x, t)$ and $j(x, t)$ coupled at every point of space and time via the continuity equation, $\partial_t \rho + \partial_x j = 0$. Moreover, the density and current fields are further constrained to yield empirical values

$$q = \frac{1}{\tau} \int_0^\tau dt \int_0^1 dx j(x, t), \quad (\text{S79})$$

$$m = \frac{1}{\tau} \int_0^\tau dt \int_0^1 dx \rho(x, t), \quad (\text{S80})$$

and boundary conditions for the density field are such that $\rho(0, t) = \rho_L$ and $\rho(1, t) = \rho_R \forall t$. We have seen in previous sections of the SM that, under the additivity conjecture [2], the joint mass-current LDF is simplified to

$$G_{\text{ad}}(m, q) = \min_{\rho(x)} \int_0^1 dx \frac{[q + D(\rho)\rho'(x) - \sigma(\rho)E]^2}{2\sigma(\rho)}, \quad (\text{S81})$$

with a reduced set of constraints (i.e. boundary densities, and total mass). We denote in this section as $\rho_{m,q}^{\text{ad}}(x)$ the optimal density profile responsible of a joint mass and current fluctuation under the additivity hypothesis. To search for violations of the additivity principle, we focus our attention in current fluctuations $|q| \leq q_c$ below the critical point in systems driven by a *symmetric* density gradient ($\rho_R = 1 - \rho_L$). In this regime we conjecture a solution for the optimal *trajectory* responsible of a given mass-current fluctuation, which is time-dependent for masses where $G(m, q)$ is non-convex. In particular, our ansatz in this regime is

$$\rho_{m,q}(x, t) = \begin{cases} \rho_{m,q}^{\text{ad}}(x) & \text{if } m < m_q^- \text{ or } m > m_q^+ \\ \rho_{m_q^-, q}^{\text{ad}}(x) [1 - \phi(t - t_{m,q})] + \rho_{m_q^+, q}^{\text{ad}}(x) \phi(t - t_{m,q}) & \text{if } m_q^- \leq m \leq m_q^+ \end{cases} \quad (\text{S82})$$

where m_q^\pm are the masses of the optimal density profiles associated to a current fluctuation $|q| \leq q_c$ in the PH symmetry broken regime along the high-mass (+) and low-mass (-) branches. The time-dependent function $\phi(t)$ is a sufficiently smooth localized crossover function such that $\phi(t) = 0 \forall t < -\frac{\delta t}{2}$ and $\phi(t) = 1 \forall t > \frac{\delta t}{2}$, with δt a fixed timescale. The crossover time $t_{m,q}$ in Eq (S82) can be determined now by imposing the constraint on the empirical mass, Eq. (S80). In particular

$$\begin{aligned} m &= \frac{1}{\tau} \int_0^\tau dt \int_0^1 dx \rho_{m,q}(x, t) = \left(\frac{t_{m,q} - \frac{\delta t}{2}}{\tau} \right) m_q^- + \left(\frac{\tau - (t_{m,q} + \frac{\delta t}{2})}{\tau} \right) m_q^+ + \frac{1}{\tau} \int_{t_{m,q} - \frac{\delta t}{2}}^{t_{m,q} + \frac{\delta t}{2}} dt \int_0^1 dx \rho_{m,q}(x, t) \\ &= \frac{t_{m,q}}{\tau} m_q^- + \left(1 - \frac{t_{m,q}}{\tau} \right) m_q^+ + \frac{1}{\tau} \left[-\delta t + \int_{t_{m,q} - \frac{\delta t}{2}}^{t_{m,q} + \frac{\delta t}{2}} dt \int_0^1 dx \rho_{m,q}(x, t) \right]. \end{aligned} \quad (\text{S83})$$

The third term in the rhs of the last equation is $\sim \mathcal{O}(\delta t/\tau)$, so in the long-time limit ($\tau \rightarrow \infty$) and for a fixed crossover time δt this term tends to zero, and hence we find $t_{m,q} = p \tau$ with the definition

$$p = \frac{m_q^+ - m}{m_q^+ - m_q^-}. \quad (\text{S84})$$

As mentioned above, the time-dependent optimal density field $\rho_{m,q}(x, t)$ must obey at all points of space and time a continuity equation $\partial_t \rho_{m,q}(x, t) + \partial_x j_{m,q}(x, t) = 0$. To obtain the optimal time-dependent current field $j_{m,q}(x, t)$

for $m_q^- \leq m \leq m_q^+$, we first note that in this case

$$\partial_t \rho_{m,q}(x,t) = \begin{cases} 0 & \text{if } t \notin [t_{m,q} - \frac{\delta t}{2}, t_{m,q} + \frac{\delta t}{2}] \\ \left[\rho_{m_q^+,q}^{\text{ad}}(x) - \rho_{m_q^-,q}^{\text{ad}}(x) \right] \phi'(t - t_{m,q}) & \text{if } t \in [t_{m,q} - \frac{\delta t}{2}, t_{m,q} + \frac{\delta t}{2}] \end{cases} \quad (\text{S85})$$

Therefore the continuity constraint in the mass regime $m_q^- \leq m \leq m_q^+$ leads to the following optimal current trajectory

$$j_{m,q}(x,t) = \begin{cases} q & \text{if } t \notin [t_{m,q} - \frac{\delta t}{2}, t_{m,q} + \frac{\delta t}{2}] \\ \chi(x) \phi'(t - t_{m,q}) & \text{if } t \in [t_{m,q} - \frac{\delta t}{2}, t_{m,q} + \frac{\delta t}{2}] \end{cases} \quad (\text{S86})$$

where we have already taken into account the constraint on the empirical current q , see Eq. (S79). The function $\chi(x)$ is such that $\chi'(x) = \rho_{m_q^+,q}^{\text{ad}}(x) - \rho_{m_q^-,q}^{\text{ad}}(x)$, and we note that the transient regime where $j_{m,q}(x,t)$ is different from q does not contribute to the final value of the empirical current, Eq. (S79), as this transient is negligible against the long-time limit for τ .

Using this ansatz for the optimal trajectory responsible of a mass and current fluctuation in Eq. (S78), we obtain for the associated joint LDF

$$\begin{aligned} G(m,q) &= \lim_{\tau \rightarrow \infty} \frac{1}{\tau} \int_0^\tau dt \int_0^1 dx \frac{[j_{m,q}(x,t) + D(\rho_{m,q}) \partial_x \rho_{m,q}(x,t) - E\sigma(\rho_{m,q})]^2}{2\sigma(\rho_{m,q})} \\ &= \lim_{\tau \rightarrow \infty} \left[\left(\frac{t_{m,q} - \frac{\delta t}{2}}{\tau} \right) G_{\text{ad}}(m_q^-, q) + \left(\frac{\tau - (t_{m,q} + \frac{\delta t}{2})}{\tau} \right) G_{\text{ad}}(m_q^+, q) + \frac{1}{\tau} \mathcal{I} \right], \end{aligned} \quad (\text{S87})$$

with the definition

$$\mathcal{I} \equiv \int_{t_{m,q} - \frac{\delta t}{2}}^{t_{m,q} + \frac{\delta t}{2}} dt \int_0^1 dx \frac{[j_{m,q}(x,t) + D(\rho_{m,q}) \partial_x \rho_{m,q}(x,t) - E\sigma(\rho_{m,q})]^2}{2\sigma(\rho_{m,q})}. \quad (\text{S88})$$

Noting that $\mathcal{I} \sim \mathcal{O}(\delta t)$ and using the same arguments as above, we find in the long-time limit $\tau \rightarrow \infty$ that

$$G(m,q) = p G_{\text{ad}}(m_q^-, q) + (1-p) G_{\text{ad}}(m_q^+, q), \quad (\text{S89})$$

which corresponds to the Maxwell construction obtained from $G_{\text{ad}}(m,q)$ in the mass regime $m_q^- \leq m \leq m_q^+$ where this joint LDF is non-convex (for $|q| \leq q_c$), as described above and in the main text. Note that an equivalent argument can be developed for the conditional mass-current LDF $G(m|q) = G(m,q) - G(q)$. This instanton solution corresponds to the dynamical coexistence of the different symmetry-broken phases which appear for $|q| \leq q_c$, a behavior typical of 1st-order DPTs. Note also that one can generalize the previous solution to PH-asymmetric boundaries in regimes where $G(m,q)$ is non-convex. Finally, we would like to mention that some subtleties of the instanton solution appear for $|q| \approx q_c$ related to the order of the $L \rightarrow \infty$ and $\tau \rightarrow \infty$ limits, see Ref. [22] for a discussion of this issue.

V. SPECTRAL ANALYSIS OF THE DYNAMICAL GENERATOR AND METASTABLE MANIFOLD

In this section we perform a spectral analysis of the microscopic dynamics of the $1d$ WASEP in order to better understand the DPT demonstrated above from a microscopic point of view. In particular, we will focus on the quasi-degenerate (metastable) states $|P_{MS}^{c_1}\rangle$ and $|P_{MS}^{c_2}\rangle$ introduced in the main text, which contain the information about the optimal trajectories in the symmetry-broken phase.

At the microscopic level, a configuration of the $1d$ WASEP is given by $C = \{n_k\}_{k=1,\dots,L}$, where $n_k = 0, 1$ is the occupation number of the k^{th} -site of the lattice. Within the quantum Hamiltonian formalism for the master equation [23], each configuration is then represented as a vector in a Hilbert space

$$|C\rangle = \bigotimes_{k=1}^L \begin{pmatrix} n_k \\ 1 - n_k \end{pmatrix}, \quad (\text{S90})$$

and the complete information about the system is contained in a vector $|P\rangle = (P(C_1), P(C_2), \dots)^T = \sum_i P(C_i) |C_i\rangle$, with T denoting transposition, such that $P(C_i)$ represents the probability of configuration C_i . This probability vector is normalized such that $\langle -|P\rangle = 1$ where $\langle -| = \sum_i \langle C_i|$ is the vector representing the sum over all possible configurations and $\langle C_i|C_j\rangle = \delta_{ij}$. The probability vector $|P\rangle$ evolves in time according to the master equation

$$\partial_t |P\rangle = \mathbb{W} |P\rangle, \quad (\text{S91})$$

where \mathbb{W} defines the Markov generator of the dynamics. Such generator can be *tilted* $\mathbb{W}^{\mu,\lambda}$ [6, 25] to bias the original stochastic dynamics in order to favor large (low) mass for $\mu < 0$ ($\mu > 0$) and large (low) currents for $\lambda > 0$ ($\lambda < 0$), with μ and λ the conjugate parameters to the microscopic mass and current observables, respectively. In particular, the tilted dynamical generator for the $1d$ open WASEP is

$$\begin{aligned} \mathbb{W}^{\mu,\lambda} = & \sum_{k=1}^{L-1} \left[\frac{1}{2} e^{(\lambda+E)/(L-1)} \sigma_{k+1}^+ \sigma_k^- + \frac{1}{2} e^{-(\lambda+E)/(L-1)} \sigma_k^+ \sigma_{k+1}^- \right. \\ & - \frac{1}{2} e^{E/(L-1)} \hat{n}_k (\mathbb{1} - \hat{n}_{k+1}) - \frac{1}{2} e^{-E/(L-1)} \hat{n}_{k+1} (\mathbb{1} - \hat{n}_k) \\ & + \alpha [\sigma_1^+ - (\mathbb{1} - \hat{n}_1)] + \gamma [\sigma_1^- - \hat{n}_1] \\ & \left. + \delta [\sigma_L^+ - (\mathbb{1} - \hat{n}_L)] + \beta [\sigma_L^- - \hat{n}_L] - \frac{\mu}{L} \sum_{k=1}^L \hat{n}_k \right], \end{aligned} \quad (\text{S92})$$

and we recall (see main text) that α and γ (δ and β) are the injection and extraction rates at the leftmost (rightmost) site, respectively. In the previous expression $\mathbb{1}$ is the identity matrix and $\hat{n}_k = \sigma_k^+ \sigma_k^-$ is the number operator at site $k \in [1, L]$, where σ_k^+ and σ_k^- are the creation and annihilation operators given by $\sigma_k^\pm = (\sigma_k^x \pm i\sigma_k^y)/2$ respectively, with $\sigma_k^{x,y}$ the standard x, y -Pauli matrices acting on site k . The connection between the biased dynamics and the large deviation properties of the $1d$ WASEP is established through the largest eigenvalue of $\mathbb{W}^{\mu,\lambda}$ [25, 26]. Such eigenvalue, denoted by $\theta_0(\mu, \lambda)$, is nothing but the cumulant generating function of the observables m and q , related to the LDF $G(m, q)$ via a Legendre transform,

$$\theta_0(\mu, \lambda) = L^{-1} \max_{m,q} [\lambda q - \mu L m - G(m, q)]. \quad (\text{S93})$$

The average of an observable b at a final time t in the unbiased ($\lambda = \mu = 0$) dynamics can be written in operator notation as $\langle b(t) \rangle \equiv \langle -|\hat{b} e^{t\mathbb{W}^{0,0}}|P_0\rangle$. We can write the time evolution operator for long times as $e^{t\mathbb{W}^{0,0}} \sim |P_{ss}\rangle \langle -|$, with $|P_{ss}\rangle$ being the stationary state probability vector. Thus, as $\langle -|P_0\rangle = 1$ the average of b is $\langle b(t) \rangle \equiv \langle -|\hat{b}|P_{ss}\rangle$. Since we are in the unbiased dynamics this average is the same at both the final time t and the intermediate times $0 \ll \tau \ll t$, so that $\langle b(t) \rangle = \langle b(\tau) \rangle$ [27]. However, for a biased dynamics such as $\mathbb{W}^{0,\lambda}$, we are interested in computing the average of observables at intermediate times, since the rare event sustained by $\mathbb{W}^{0,\lambda}$ presents time-boundary effects which make the average at final and at intermediate times no longer equivalent [27]. Hence, in order to make these averages equivalent in the biased dynamics, we transform the non-stochastic generator $\mathbb{W}^{0,\lambda}$ (note that it does not conserve probability $\langle -|\mathbb{W}^{0,\lambda} \neq 0$) into a physical stochastic generator via the Doob transform [28, 29]:

$$\mathbb{W}_{Dob}^{0,\lambda} = \hat{L}_0 \mathbb{W}^{0,\lambda} \hat{L}_0^{-1} - \theta_0(\lambda), \quad (\text{S94})$$

which is a proper stochastic generator (now $\langle -|\mathbb{W}_{Dob}^{0,\lambda} = 0$), with largest eigenvalue equal to zero, generating the same trajectories as $\mathbb{W}^{0,\lambda}$. Here \hat{L}_0 is a diagonal matrix whose elements $(\hat{L}_0)_{ii}$ are the i -th entries of the left eigenvector

$\langle L_0|$ of the biased generator $\mathbb{W}^{0,\lambda}$ associated with its largest eigenvalue $\theta_0(\lambda)$. Thus, with this new generator $\mathbb{W}_{Doob}^{0,\lambda}$ we can compute the average of any observable b at intermediate times as

$$\langle b(\tau) \rangle_\lambda = \langle b(t) \rangle_\lambda \equiv \frac{\langle -|\hat{b}e^{t\mathbb{W}_{Doob}^{0,\lambda}}|P_0\rangle}{\langle -|e^{t\mathbb{W}_{Doob}^{0,\lambda}}|P_0\rangle}. \quad (\text{S95})$$

In what follows we show how the previous average takes different forms depending on whether or not the largest eigenvalue of the biased generator $\mathbb{W}^{0,\lambda}$ is degenerate.

A. Non-degenerate largest eigenvalue (PH symmetric phase)

If $\theta_0(\lambda)$ is non-degenerate, the time evolution operator for long times is $e^{t\mathbb{W}^{0,\lambda}} \sim e^{t\theta_0(\lambda)} |R_0\rangle \langle L_0|$. Then by using (S94) the asymptotic Doob time evolution operator reads

$$e^{t\mathbb{W}_{Doob}^{0,\lambda}} \sim \hat{L}_0 |R_0\rangle \langle L_0| \hat{L}_0^{-1} = \hat{L}_0 |R_0\rangle \langle -|,$$

with $|R_0\rangle$ being the right eigenvector of $\mathbb{W}^{0,\lambda}$ associated with its largest eigenvalue $\theta_0(\lambda)$. Additionally we can normalize eigenvectors so that

$$\langle L_i|R_j\rangle = \delta_{ij} \quad \text{and} \quad \langle -|R_0\rangle = 1.$$

Thus the time-evolved initial probability vector is

$$e^{t\mathbb{W}_{Doob}^{0,\lambda}}|P_0\rangle \sim \hat{L}_0 |R_0\rangle. \quad (\text{S96})$$

As a consequence the average (S95) is given by

$$\langle b(\tau) \rangle_\lambda = \frac{\langle -|\hat{b}\hat{L}_0 |R_0\rangle}{\langle -|\hat{L}_0 |R_0\rangle} = \frac{\langle -|\hat{b}\hat{L}_0 |R_0\rangle}{\langle L_0|R_0\rangle} = \langle -|\hat{b}\hat{L}_0 |R_0\rangle$$

where in the last equality we have used the fact that eigenvectors are normalized. This is how we calculate, from the microscopic dynamics, the optimal density profiles associated with current fluctuations ($\lambda \neq 0$) in the particle-hole (PH) symmetric phase. The optimal particle density in the large size limit at $x = k/L$, with L being the total number of sites, is thus given by

$$\rho(x) = \langle \hat{n}_k(\tau) \rangle_\lambda = \langle -|\hat{n}_k\hat{L}_0 |R_0\rangle.$$

B. Degenerate largest eigenvalue (PH symmetry-broken phase)

As we have seen in the main text, for $\lambda_c^- \leq \lambda \leq \lambda_c^+$ (or equivalently $|q| \leq q_c$), the largest eigenvalue of $\mathbb{W}^{0,\lambda}$ becomes degenerate in the large size limit, $L \rightarrow \infty$. This is reflected in the diffusively-scaled spectral gap, $L^2[\theta_0(0,\lambda) - \theta_1(0,\lambda)]$, with $\theta_1(0,\lambda)$ the next-to-leading eigenvalue of $\mathbb{W}^{0,\lambda}$, which tends to zero as L increases in this λ -region. In this case, defining as $|R_1\rangle$ and $\langle L_1|$ the right and left eigenvectors associated to $\theta_1(0,\lambda)$, we have that the time evolution operator can be written for long times as $e^{t\mathbb{W}^{0,\lambda}} \sim e^{t\theta_0(\lambda)}(|R_0\rangle \langle L_0| + |R_1\rangle \langle L_1|)$. Hence, by using (S94) the asymptotic Doob time evolution operator reads

$$e^{t\mathbb{W}_{Doob}^{0,\lambda}} \sim \hat{L}_0 |R_0\rangle \langle L_0| \hat{L}_0^{-1} + \hat{L}_0 |R_1\rangle \langle L_1| \hat{L}_0^{-1} = \hat{L}_0 |R_0\rangle \langle -| + \hat{L}_0 |R_1\rangle \langle L_1| \hat{L}_0^{-1}.$$

Thus the time-evolved initial vector probability is

$$\boxed{e^{t\mathbb{W}_{Doob}^{0,\lambda}}|P_0\rangle \sim \hat{L}_0 |R_0\rangle + c\hat{L}_0 |R_1\rangle}, \quad (\text{S97})$$

with $c = \langle L_1|\hat{L}_0^{-1}|P_0\rangle$. Note that, since $\langle -|P_0\rangle = 1$ then $c \in [c_1, c_2]$ with $c_1 = \min(\langle L_1|\hat{L}_0^{-1})$ and $c_2 = \max(\langle L_1|\hat{L}_0^{-1})$, where min and max correspond to the minimum and maximum entries of the vector $\langle L_1|\hat{L}_0^{-1}$.

Thus, Eq. (S97) defines the set of metastable states $|P_{MS}^c\rangle$ of the main text, whose extremes are given by $|P_{MS}^{c_1}\rangle$ and $|P_{MS}^{c_2}\rangle$. As a consequence the average (S95) is given by

$$\langle b(\tau) \rangle_\lambda = \frac{\langle -|\hat{b}\hat{L}_0|R_0\rangle + c\langle -|\hat{b}\hat{L}_0|R_1\rangle}{\langle -|\hat{L}_0|R_0\rangle + c\langle -|\hat{L}_0|R_1\rangle} = \langle -|\hat{b}\hat{L}_0|R_0\rangle + c\langle -|\hat{b}\hat{L}_0|R_1\rangle$$

where in the last equality we have used the fact that eigenvectors are normalized. This is how we calculate, from the microscopic dynamics, the optimal density profiles associated with current fluctuations ($\lambda \neq 0$) in the symmetry-broken phase. The optimal particle densities in the large size limit at $x = k/L$, are thus given by

$$\rho_1(x) = \langle \hat{n}_k(\tau) \rangle_\lambda = \langle -|\hat{n}_k\hat{L}_0|R_0\rangle + c_1\langle -|\hat{n}_k\hat{L}_0|R_1\rangle$$

and

$$\rho_2(x) = \langle \hat{n}_k(\tau) \rangle_\lambda = \langle -|\hat{n}_k\hat{L}_0|R_0\rangle + c_2\langle -|\hat{n}_k\hat{L}_0|R_1\rangle ,$$

which correspond to the metastable density profiles for $L = 10$ and $L = 20$ of Fig. 4 in the main text.

-
- [1] L. Bertini, A. De Sole, D. Gabrielli, G. Jona-Lasinio, and C. Landim, “Macroscopic fluctuation theory,” *Rev. Mod. Phys.* **87**, 593–636 (2015).
 - [2] T. Bodineau and B. Derrida, “Current fluctuations in nonequilibrium diffusive systems: An additivity principle,” *Phys. Rev. Lett.* **92**, 180601 (2004).
 - [3] B. Derrida, “An exactly soluble non-equilibrium system: The asymmetric simple exclusion process,” *Phys. Rep.* **301**, 65–83 (1998).
 - [4] T. Chou, K. Mallick, and R. K. P. Zia, “Non-equilibrium statistical mechanics: from a paradigmatic model to biological transport,” *Reports On Progress In Phys.* **74**, 116601 (2011).
 - [5] B. Derrida, “Non-equilibrium steady states: fluctuations and large deviations of the density and of the current,” *J. Stat. Mech.* P07023 (2007).
 - [6] P. I. Hurtado, C. P. Espigares, J. J. del Pozo, and P. L. Garrido, “Thermodynamics of currents in nonequilibrium diffusive systems: theory and simulation,” *J. Stat. Phys.* **154**, 214–264 (2014).
 - [7] L. Bertini, A. De Sole, D. Gabrielli, G. Jona-Lasinio, and C. Landim, “Current fluctuations in stochastic lattice gases,” *Phys. Rev. Lett.* **94**, 030601 (2005).
 - [8] L. Bertini, A. De Sole, D. Gabrielli, G. Jona-Lasinio, and C. Landim, “Nonequilibrium current fluctuations in stochastic lattice gases,” *J. Stat. Phys.* **123**, 237–276 (2006).
 - [9] P. I. Hurtado and P. L. Garrido, “Current fluctuations and statistics during a large deviation event in an exactly solvable transport model,” *J. Stat. Mech.* P02032 (2009).
 - [10] P. I. Hurtado and P. L. Garrido, “Spontaneous symmetry breaking at the fluctuating level,” *Phys. Rev. Lett.* **107**, 180601 (2011).
 - [11] K. Saito and A. Dhar, “Additivity principle in high-dimensional deterministic systems,” *Phys. Rev. Lett.* **107**, 250601 (2011).
 - [12] P. I. Hurtado, C. Pérez-Espigares, J. J. del Pozo, and P. L. Garrido, “Symmetries in fluctuations far from equilibrium,” *Proc. Natl. Acad. Sci. USA* **108**, 7704–7709 (2011).
 - [13] C. Pérez-Espigares, P. L. Garrido, and P. I. Hurtado, “Dynamical phase transition for current statistics in a simple driven diffusive system,” *Phys. Rev. E* **87**, 032115 (2013).
 - [14] P. I. Hurtado, A. Lasanta, and A. Prados, “Typical and rare fluctuations in nonlinear driven diffusive systems with dissipation,” *Phys. Rev. E* **88**, 022110 (2013).
 - [15] M. Žnidarič, “Exact large-deviation statistics for a nonequilibrium quantum spin chain,” *Phys. Rev. Lett.* **112**, 040602 (2014).
 - [16] O. Shpielberg and E. Akkermans, “Le Chatelier principle for out-of-equilibrium and boundary-driven systems: Application to dynamical phase transitions,” *Phys. Rev. Lett.* **116** (2016).
 - [17] C. Pérez-Espigares, P. L. Garrido, and P. I. Hurtado, “Weak additivity principle for current statistics in d -dimensions,” *Phys. Rev. E* **93**, 040103(R) (2016).
 - [18] N. Tizón-Escamilla, P. I. Hurtado, and P. L. Garrido, “Structure of the optimal path to a fluctuation,” *Phys. Rev. E* **95**, 002100 (2017).
 - [19] N. Tizón-Escamilla, C. Pérez-Espigares, P. L. Garrido, and P. I. Hurtado, “Order and symmetry breaking in the fluctuations of driven systems,” *Phys. Rev. Lett.* **119**, 090602 (2017).
 - [20] Y. Baek, Y. Kafri, and V. Lecomte, “Dynamical symmetry breaking and phase transitions in driven diffusive systems,” *Phys. Rev. Lett.* **118**, 030604 (2017).
 - [21] P. F. Byrd and M. D. Friedman, *Handbook of Elliptic Integrals for Engineers and Scientists* (Springer-Verlag, 1971).

- [22] Y. Baek, Y Kafri, and Lecomte V., “Dynamical phase transitions in the current distribution of driven diffusive channels,” *J. Phys. A* **51**, 105001 (2018).
- [23] G. M. Schutz, *Exactly solvable models for many-body systems far from equilibrium*, Vol. 19 (2001) pp. 1–251.
- [25] H. Touchette, “The large deviation approach to statistical mechanics,” *Phys. Rep.* **478**, 1–69 (2009).
- [26] J. P. Garrahan, “Aspects of non-equilibrium in classical and quantum systems: Slow relaxation and glasses, dynamical large deviations, quantum non-ergodicity, and open quantum dynamics,” *Physica A* **504**, 130 (2018).
- [27] J. P. Garrahan, R. L. Jack, V. Lecomte, E. Pitard, K. van Duijvendijk, and F. van Wijland, “First-order dynamical phase transition in models of glasses: an approach based on ensembles of histories,” *J. Phys. A* **42**, 075007 (2009).
- [28] R. Chetrite and H. Touchette, “Variational and optimal control representations of conditioned and driven processes,” *J. Stat. Mech.* P12001 (2015).
- [29] F. Carollo, J. P. Garrahan, I. Lesanovsky, and C. Pérez-Espigares, “Making rare events typical in markovian open quantum systems,” *Phys. Rev. A* **98**, 010103 (2018).